Journal of Computational Physics 231 (2012) 2482–2497

Contents lists available at SciVerse ScienceDirect

Journal of Computational Physics

journal homepage: www.elsevier.com/locate/jcp

Numerical methods for stochastic partial differential equations with multiple scales

A. Abdulle [a], G.A. Pavliotis [b,*]

[a] Mathematics Section, Ecole Polytechnique Fédérale de Lausanne, CH-1015 Lausanne, Switzerland
[b] Department of Mathematics, Imperial College London, London SW7 2AZ, UK

ARTICLE INFO

Article history:
Received 23 May 2011
Received in revised form 3 October 2011
Accepted 27 November 2011
Available online 13 December 2011

Keywords:
Stochastic partial differential equations
Multiscale methods
Averaging
Homogenization
Heterogeneous multiscale method (HMM)

ABSTRACT

A new method for solving numerically stochastic partial differential equations (SPDEs) with multiple scales is presented. The method combines a spectral method with the heterogeneous multiscale method (HMM) presented in [W. E, D. Liu, E. Vanden-Eijnden, Analysis of multiscale methods for stochastic differential equations, Commun. Pure Appl. Math., 58(11) (2005) 1544–1585]. The class of problems that we consider are SPDEs with quadratic nonlinearities that were studied in [D. Blömker, M. Hairer, G.A. Pavliotis, Multiscale analysis for stochastic partial differential equations with quadratic nonlinearities, Nonlinearity, 20(7) (2007) 1721–1744]. For such SPDEs an amplitude equation which describes the effective dynamics at long time scales can be rigorously derived for both advective and diffusive time scales. Our method, based on micro and macro solvers, allows to capture numerically the amplitude equation accurately at a cost independent of the small scales in the problem. Numerical experiments illustrate the behavior of the proposed method.

1. Introduction

Many interesting phenomena in the physical sciences and in applications are characterized by their high dimensionality and the presence of many different spatial and temporal scales. Standard examples include atmosphere and ocean sciences [1], molecular dynamics [2] and materials science [3]. The mathematical description of phenomena of this type quite often leads to infinite dimensional multiscale systems that are described by nonlinear evolution partial differential equations (PDEs) with multiple scales.

Often physical systems are also subject to noise. This noise might be either due to thermal fluctuations [4], noise in some control parameter [5], coarse-graining of a high-dimensional deterministic system with random initial conditions [6,7], or the stochastic parameterization of small scales [8]. High dimensional multiscale dynamical systems that are subject to noise can be modeled accurately using stochastic partial differential equations (SPDEs) with a multiscale structure. As examples of mathematical modeling using SPDEs we mention the stochastic Navier–Stokes equations [9] that arise in the study of hydrodynamic fluctuations, the stochastic Swift–Hohenberg and stochastic Kuramoto–Shivashinsky equation that arise in the study of pattern formation [10], the Langevin-type SPDEs that arise in path sampling and Markov Chain Monte Carlo in infinite dimensional dimensions [11] and the stochastic KPZ equation that is used in the modeling of the evolution of growing interfaces. Most of the equations mentioned above are semilinear parabolic equations with quadratic nonlinearities for which the numerical algorithm proposed in this paper can be applied, in principle.

* Corresponding author.
E-mail address: g.pavliotis@imperial.ac.uk (G.A. Pavliotis).

0021-9991/$ - see front matter © 2011 Elsevier Inc. All rights reserved.
doi:10.1016/j.jcp.2011.11.039

There are very few instances where SPDEs with multiple scales can be treated analytically. The goal of this paper is to develop numerical methods for solving accurately and efficiently multiscale SPDEs. Several numerical methods for SPDEs have been developed and analyzed in recent years, e.g. [12–14], based on a finite difference scheme in both space and time. It is well known that explicit time discretization via standard methods (e.g., as the Euler–Maruyama method) leads to a time-step restriction due to the stiffness originating from the discretisation of the diffusion operator (e.g. the Courant–Friedrichs–Lewy (CFL) condition $\Delta t \leqslant C(\Delta x)^2$, where Δt and Δx are the time and space discretization, respectively). The situation is even worse for SPDEs with multiple scales (e.g. of the form (3) and (4) below) as in this case the CFL condition becomes $\Delta t \leqslant C(\Delta x \cdot \epsilon)^2$, where $\epsilon \ll 1$ is the parameter measuring scale separation. Standard explicit methods become useless for SPDEs with multiple scales.

Such time-step restriction can in theory be removed by using implicit methods as was shown in [14]. However the implicitness of the numerical scheme forces one to solve potentially large linear algebraic problems at each time step. Furthermore, it was shown in [15] that implicit methods are not suited for studying the long time dynamics of fast–slow stochastic systems as they do not capture the correct invariant measure of the system. Although this result has been obtained for finite dimensional stochastic systems, it is expected that it also applies to infinite dimensional fast–slow systems of stochastic differential equations (SDEs), rendering the applicability of implicit methods to SPDEs with multiple scales questionable. We also note that a new class of explicit methods, the S-ROCK methods, with much better stability properties than the Euler–Maruyama method was recently introduced in [16–18]. Although these methods are much more efficient than traditional explicit methods, computing time issues will occur when trying to solve SPDEs with multiple scales as considered here, since the stiffness is extremely severe for small ϵ. Furthermore, capturing the correct invariant measure of the SPDE for $\Delta t > \epsilon$ is still an issue for such solvers.

In this paper we consider SPDEs of the form

$$\partial_t v = \mathcal{A} v + F(v) + \epsilon Q \xi, \tag{1}$$

posed in a bounded domain of $\mathbb{R}$ with appropriate boundary conditions. The differential operator $\mathcal{A}$ is assumed to be a non-positive self-adjoint operator in a Hilbert space $\mathcal{H}$ with compact resolvent, ξ denotes space-time Gaussian white noise, Q is the covariance operator of the noise and we take $\epsilon \ll 1$. We assume that the operator $\mathcal{A}$ and the covariance operator of the noise Q commute, and that $\mathcal{A}$ has a finite dimensional kernel.[1]

The finite dimensional kernel of the operator $\mathcal{A}$ leads to scale separation between the slow dynamics in $\mathcal{N}$ and the fast dynamics in the orthogonal complement of the null space $\mathcal{N}^\perp$, where $\mathcal{H} = \mathcal{N} \oplus \mathcal{N}^\perp$. In this paper we will furthermore assume that noise acts directly only on the orthogonal complement $\mathcal{N}^\perp$. This assumption is consistent with the scaling of the noise in (1), i.e. that it is of $O(\epsilon)$, and it leads to the singularly perturbed SPDEs (3) and (4) below. When noise acts also on the slow variables, then, its amplitude has to be scaled differently in Eq. (1); in particular it has to be of $O(\epsilon^2)$. In this case, and after rescaling in time, we end up with a non-singularly perturbed equation for which the analysis is easier. A problem of this type has been studied and the amplitude equation has been derived in [39].

For concreteness, we will focus on the class of SPDEs with quadratic nonlinearities that was considered in [19], and assume that

$$F(u) = f(u) + \epsilon^\alpha g(u), \tag{2}$$

where f is a quadratic function (e.g. $f(u) = B(u,u)$, a symmetric bilinear form), g a linear function and the exponent α is either 1 or 2.[2] The choice of α will depend on the particular scaling. In order to describe the longtime behavior of the SPDEs we perform an *advective* rescaling set $v(t) := \epsilon u(\epsilon t)$. Using the scaling properties of white noise and (2) with $\alpha = 1$ we obtain the following singularly perturbed SPDE

$$\partial_t u = \frac{1}{\epsilon}\mathcal{A} u + F(u) + \frac{1}{\sqrt{\epsilon}} Q \xi. \tag{3}$$

Another scaling is of interest, namely the *diffusive* rescaling $v(t) := \epsilon u(\epsilon^2 t)$ which, for (2) with $\alpha = 2$ leads to the SPDE

$$\partial_t u = \frac{1}{\epsilon^2}\mathcal{A} u + \frac{1}{\epsilon} F(u) + \frac{1}{\epsilon} Q \xi. \tag{4}$$

Alternatively, one can start with the singularly perturbed SPDEs (3) and (4) without any reference to the SPDE (1).

Singularly perturbed SPDEs with quadratic nonlinearities provide a natural testbed for testing the applicability of the heterogeneous multiscale method to infinite dimensional stochastic systems, since a rigorous homogenization theory exists for this class of SPDEs [19]. Furthermore, SPDEs of this form arise naturally in stochastic models for climate [1] and in surface growth [21,22]. Finally, it has already been shown through rigorous analysis and numerical experiments that these systems exhibit a very rich dynamical behavior, such as noise-induced transitions [23] and the possibility of stabilization of linearly

[1] Notice that the compactness of the resolvent of $\mathcal{A}$ implies that the operator has discrete spectrum which, together with the self-adjointness of $\mathcal{A}$ and the assumption that it commutes with the covariance operator of the noise Q, allow to expand the solution of (1) in terms of the eigenfunctions of $\mathcal{A}$.

[2] Usually the functions f and g involve derivatives of the function u. For example, for both the Burgers and the Kuramoto–Shivashinsky equation we have $f(u) = u\partial_x u$. The linear function $g(u)$ is included to induce a linear instability to the dynamics. In the case of the Burgers equation we will simply take $g(u) = u$ whereas in the case of the Kuramoto–Shivashinsky equation we can take $g(u) = \partial_x^4 u$. Further discussion can be found in Section 4 and in [20].

unstable modes due to the interaction between the additive noise and the scale separation [24,20]. We believe, however, that the methodology developed in this paper has a wider range of applicability and is not restricted to SPDEs with quadratic nonlinearities. Further comments about the class of SPDEs for which we believe that the proposed numerical method can be applied can be found in Section 5.

Our numerical algorithm is based on a combination of a spectral method with micro-macro time integration schemes. We denote by $x = \mathcal{P}_c u$ the projection onto $\mathcal{N}$ and by $y = \mathcal{P}_s u,\ P_s = I - \mathcal{P}_c$ the projection onto $\mathcal{N}^\perp$. We then rewrite (3) and (4) as fast–slow system of SDEs

$$\dot{x} = a(x,y), \tag{5a}$$

$$\dot{y} = \frac{1}{\epsilon}\mathcal{A}y + b(x,y) + \frac{1}{\sqrt{\epsilon}}Q\xi \tag{5b}$$

and

$$\dot{x} = \frac{1}{\epsilon}a(x,y), \tag{6a}$$

$$\dot{y} = \frac{1}{\epsilon^2}\mathcal{A}y + \frac{1}{\epsilon}b(x,y) + \frac{1}{\epsilon}Q\xi, \tag{6b}$$

where the functions $a(x,y)$ and $b(x,y)$ are the projections of $F(u)$ onto $\mathcal{N}$ and $\mathcal{N}^\perp$. We emphasize the fact that the separation of scales between x and y is due to the fact that the linear operator $\mathcal{A}$ has a non-trivial null space, since $\mathcal{A}x$ is absent in Eqs. (5a) and (6a). We remark that an $\mathcal{O}(1)$ nonlinear term can be added in (6a). The fast–slow systems (5) and (6) resemble fast slow systems for SDEs [25, Ch. 10,11]. However, the fast process y is infinite dimensional and the well known averaging and homogenization theorems [26,27] do not apply.

Averaging and homogenization results for SPDEs have been obtained recently [28,19]. In particular, provided that the fast process y in (5) has suitable ergodic properties, then the slow variable x converges, in the limit as ϵ tends to 0, to the solution of the averaged equation

$$\dot{x} = \hat{a}(x), \tag{7}$$

where the averaged coefficient $\hat{a}$ is given by the average of $a(x,y)$ with respect to the invariant measure of the (infinite dimensional) fast process y. When this average vanishes (i.e. the centering condition from homogenization theory is satisfied) then the dynamics at the advective time scale becomes trivial and it is necessary to look at the dynamics at the diffusive time scale, Eqs. (6). It was shown in [19] that the slow variable x of this system of equations, the solution of (6a), converges in the limit as ϵ tends to 0 to the solution of the homogenized equation

$$\dot{x} = \bar{a}(x) + \bar{\sigma}(x)\xi, \tag{8}$$

with explicit formulas for the homogenized coefficients – see Section 3 for details. For finite dimensional fast systems, the coefficients in (7) and (8) can be calculated, in principle, in terms of appropriate long-time averages – see [25] for details. The numerical method proposed in [29] and analyzed in [8], coined under the name of the heterogeneous multiscale method (HMM), relies on the numerical approximation of the coefficients in (7) and (8) by solving the original fine scale problem on time intervals of an intermediate time scale and use that data to evolve the slow variables using either (7) or (8). In this paper we show how this methodology, when combined with a spectral method, can also be applied to SPDEs with multiple scales, that is, to the systems (5) and (6). The aim of the present paper is to present the algorithm and report numerical experiments. The analysis of the proposed numerical method and the extension to more general classes of SPDEs with multiscale structure will be presented in a forthcoming paper. The rest of the paper is organized as follows. In Section 2 we present our new algorithm. Analytical and computational techniques for the analysis of SPDEs with multiple scales at the heart of the multiscale algorithm are presented in 3. In Section 4 we present numerical experiments. Section 5 is reserved for conclusions and discussion on future work.

2. Numerical method

We propose a numerical algorithm to approximate numerically the solution of (1) based on a micro-macro algorithm, capable of capturing the effective behavior of the SPDE. We explain the numerical algorithm for the case of diffusive time scale (the hardest numerically) and comment on the advective time scale later in this section.

2.1. Multiscale algorithm

Before stating our algorithm, we first recall our main assumptions. We consider SPDEs 1 in a Hilbert space $\mathcal{H}$ with norm $\|\cdot\|$ and inner product $\langle\cdot,\cdot\rangle$. $\mathcal{A}$ denotes a differential operator, ξ space-time white noise and Q the covariance operator of the noise. We assume that $\mathcal{A}$ is a self-adjoint nonpositive operator on $\mathcal{H}$ with compact resolvent. We denote its eigenvalues and (normalized) eigenfunctions by $\{-\lambda_k, e_k\}_{k=1}^{\infty}$:

$$-\mathcal{A}e_k = \lambda_k e_k, \quad k = 1, \ldots \tag{9}$$

The eigenfunctions of $\mathcal{A}$ form an orthonormal basis in $\mathcal{H}$. We assume that $\mathcal{A}$ and the covariance operator of the noise Q commute. Thus, we can write, formally,

$$Q\xi = \sum_{k=1}^{+\infty} q_k e_k \xi_k(t), \tag{10}$$

where $\{\xi_k(t)\}_{k=1}^{+\infty}$ are independent one-dimensional white noise processes, i.e., mean-zero Gaussian processes with $\langle \xi_k(t)\xi_j(s)\rangle = \delta_{k\,j}\delta(t-s)$, $k, j = 1,2,\ldots$ Here $\delta_{k\,j}$ and $\delta(t-s)$ are the usual Kronecker delta functions.

Furthermore, we will assume that $\mathcal{A}$ has a finite dimensional kernel $\mathcal{N} := \{h \in \mathcal{H} : \mathcal{A}h = 0\}$, $\dim(\mathcal{N}) = N < +\infty$ and write $\mathcal{H} = \mathcal{N} \oplus \mathcal{N}^{\perp}$. We introduce the projection operators

$$\mathcal{P}_c : \mathcal{H} \mapsto \mathcal{N}, \tag{11a}$$

$$\mathcal{P}_s = I - \mathcal{P}_c : \mathcal{H} \mapsto \mathcal{N}^{\perp} \tag{11b}$$

and write $x := \mathcal{P}_c u$, $y := \mathcal{P}_s u$. Finally, we will assume that noise acts only on $\mathcal{N}^{\perp}$, i.e. $q_k = 0$, $k = 1\ldots,N$.

Step 1. Decomposition in a fast–slow system.

Using the projection operators defined in (11a) and (11b), Eq. (1) can be written as a fast–slow stochastic system

$$\dot{x} = \frac{1}{\epsilon}\mathcal{P}_c F(u), \tag{12a}$$

$$\dot{y} = \frac{1}{\epsilon^2}\mathcal{A}y + \frac{1}{\epsilon}\mathcal{P}_c F(u) + \frac{1}{\epsilon}Q\xi, \tag{12b}$$

where $x(t) \in \mathbb{R}^N$ since $\dim(\mathcal{N}) = N$. We order the pairs of eigenfuctions and eigenvalues such that the kernel $\mathcal{N}$ is spanned by the first N eigenfunctions of $\mathcal{A}$. We can write

$$x = \sum_{k=1}^{N} x_k e_k \quad \text{and} \quad y = \sum_{k=N+1}^{+\infty} y_k e_k.$$

We introduce the vectors $\mathbf{x} = (x_1,\ldots,x_N)$ and $\mathbf{y} = (y_{N+1},\ldots)$ containing the Fourier components (with respect to the basis $\{e_k\}_{k=1}^{\infty}$) of the functions x and y. Writing $F(u) = F(\mathbf{x},\mathbf{y})$, we further introduce

$$a^k(\mathbf{x},\mathbf{y}) := \langle F(x,y), e_k\rangle \quad \text{for } 1 \leqslant k \leqslant N, \tag{13}$$

$$b^k(\mathbf{x},\mathbf{y}) := \langle F(x,y), e_k\rangle \quad \text{for } k \geqslant N. \tag{14}$$

Remark 2.1. As mentioned in the introduction we will often consider the case $F(u) = f(u) + \epsilon^2 g(u)$. Then the above decomposition reads

$$a^k(\mathbf{x},\mathbf{y}) := \langle f, e_k\rangle + \epsilon\langle g, e_k\rangle = a_0^k(\mathbf{x},\mathbf{y}) + \epsilon a_1^k(\mathbf{x},\mathbf{y}), \tag{15}$$

$$b^k(\mathbf{x},\mathbf{y}) := \langle f, e_k\rangle + \epsilon\langle g, e_k\rangle = b_0^k(\mathbf{x},\mathbf{y}) + \epsilon b_1^k(\mathbf{x},\mathbf{y}), \tag{16}$$

where we notice that for a linear function $g(u) = vu$ we simply have $a_1^k(\mathbf{x},\mathbf{y}) = vx_k$, $b_1^k(\mathbf{x},\mathbf{y}) = vy_k$.

Then, in view of (9) and (10)we can rewrite the system (12) in the form

$$\dot{x}_k = \frac{1}{\epsilon}a^k(\mathbf{x},\mathbf{y}), \quad k = 1,\ldots N, \tag{17a}$$

$$\dot{y}_k = -\frac{1}{\epsilon^2}\lambda_k y_k + \frac{1}{\epsilon}b^k(\mathbf{x},\mathbf{y}) + \frac{1}{\epsilon}q_k\xi_k, \quad k = N+1, N+2,\ldots \tag{17b}$$

Eqs. (12), resp. (17), are the infinite system of singularly perturbed SDEs that we want to solve numerically.

Step 2. Truncation.

We consider a finite dimensional truncation of the above system and keep M fast processes[3]:

$$\dot{\mathbf{x}} = \frac{1}{\epsilon}\mathbf{a}(\mathbf{x},\mathbf{y}), \tag{18a}$$

$$\dot{\mathbf{y}} = -\frac{1}{\epsilon^2}\Lambda_M\mathbf{y} + \frac{1}{\epsilon}\mathbf{b}(\mathbf{x},\mathbf{y}) + \frac{1}{\epsilon}\mathbf{Q}_M\boldsymbol{\xi},, \tag{18b}$$

where $\mathbf{x} = (x_1,\ldots,x_N)^T$, $\mathbf{y} = (y_1,\ldots,y_M)^T$, $\boldsymbol{\xi} = (\xi_1,\ldots,\xi_M)^T$ [4] and

$$\mathbf{a}(\mathbf{x},\mathbf{y}) = (a^1(\mathbf{x},\mathbf{y}),\ldots,a^N(\mathbf{x},\mathbf{y}))^T, \tag{19}$$

$$\mathbf{b}(\mathbf{x},\mathbf{y}) = (b^1(\mathbf{x},\mathbf{y}),\ldots,b^M(\mathbf{x},\mathbf{y}))^T \tag{20}$$

[3] To simplify the notations we will use a new labeling of the index for the truncated fast system and write $(y_1,\ldots,y_M)$ instead of $(y_{N+1},\ldots,y_{N+M})$ and similarly for the nonzero eigenvalues λ_k and the nonzero noise intensity q_k.

[4] For simplicity we use the same notation $\mathbf{y}$ for the full and truncated vector containing the Fourier components of the fast process.

and $\Lambda_M = \mathrm{diag}(\lambda_1,\dots,\lambda_M)$ and $\mathbf{Q}_M = \mathrm{diag}(q_1,\dots,q_M)$. For the decomposition (16),(15), we will use the notations

$$\mathbf{a}(\mathbf{x},\mathbf{y}) = \mathbf{a}_0(\mathbf{x},\mathbf{y}) + \epsilon\mathbf{a}_1(\mathbf{x},\mathbf{y}), \tag{21}$$

$$\mathbf{b}(\mathbf{x},\mathbf{y}) = \mathbf{b}_0(\mathbf{x},\mathbf{y}) + \epsilon\mathbf{b}_1(\mathbf{x},\mathbf{y}), \tag{22}$$

where $\mathbf{a}_0,\ \mathbf{a}_1 \in \mathbb{R}^N$ and $\mathbf{b}_0,\ \mathbf{b}_1 \in \mathbb{R}^M$ with components similar as in (19) or (20).

Step 3. Numerical solution of the reduced system.

The reduced system (18) is solved by a micro-macro algorithm following [29,8]. It consists of a macrosolver chosen here to be the Euler–Maruyama scheme

$$X_{n+1} = X_n + \Delta t\bar{\mathbf{a}}_M^n + \bar{\boldsymbol{\sigma}}_M^n \Delta W_n, \tag{23}$$

where ΔW_n (the Wiener increment) is $\mathcal{N}(0,\Delta t)$ and X_n is a numerical approximation of $X(t_n)$, the solution of a homogenized problem of the type (31). Notice that Δt represents here a macrotime step, i.e., Δt can be chosen much larger than ϵ. The drift function $\bar{\mathbf{a}}_M^n \simeq \bar{bfa}_M(X_n)$ and diffusion function $\bar{\boldsymbol{\sigma}}_M^n \simeq \bar{\boldsymbol{\sigma}}_M(X_n)$ appearing in (23), recovered from a time-ensemble average, are given by

$$\begin{aligned}\bar{\mathbf{a}}_M^n = &\frac{1}{KL}\sum_{j=1}^{K}\sum_{\ell=\ell_T}^{\ell_T+L-1}\partial_y\mathbf{a}\left(X_n, Y^1_{n,\ell j}\right)Y^2_{n,\ell j}\\ &+\frac{1}{KL}\frac{\delta t}{\epsilon^2}\sum_{j=1}^{K}\sum_{\ell=\ell_T}^{n_T+L-1}\sum_{\ell'=0}^{L'}\partial_x\mathbf{a}\left(X_n, Y^1_{n,\ell+\ell' j}\right)\mathbf{a}\left(X_n, Y^1_{n,\ell j}\right),\end{aligned} \tag{24a}$$

$$\bar{\boldsymbol{\sigma}}_M^n\left(\bar{\boldsymbol{\sigma}}_M^n\right)^T = \frac{1}{KL}\frac{2\delta t}{\epsilon^2}\sum_{j=1}^{K}\sum_{\ell=\ell_T}^{\ell_T+L-1}\sum_{\ell'=0}^{L'}\mathbf{a}\left(X_n, Y^1_{n,\ell+\ell' j}\right)\otimes\mathbf{a}\left(X_n, Y^1_{n,\ell j}\right), \tag{24b}$$

where Y^1, Y^2 are the solutions of a suitable auxiliary system (given in (25) below) involving the fast problem (18b). Here K denotes the number of samples taken for the numerical calculation, L, L' the number of micro timesteps and ℓ_T a number of initial micro timesteps that are omitted in the averaging processes to reduce the effect of transients (see below).

Auxiliary system. As observed in [29], for diffusive timescales, computing effective coefficients via time-averaging (relying on ergodicity), may require to solve (18b) over time $T = \mathcal{O}(\varepsilon^{-2})$. To overcome this problem, it was suggested again in [29] to replace the fast process in (18b) by ($\mathbf{y} \simeq \mathbf{y}^1 + \varepsilon\mathbf{y}^2$)

$$\dot{\mathbf{y}}^1 = -\frac{1}{\epsilon^2}\Lambda_M\mathbf{y}^1 + \frac{1}{\epsilon}Q_M\boldsymbol{\xi}, \tag{25a}$$

$$\dot{\mathbf{y}}^2 = -\frac{1}{\epsilon^2}\Lambda_M\mathbf{y}^2 + \frac{1}{\epsilon^2}\mathbf{b}(\mathbf{x},\mathbf{y}^1). \tag{25b}$$

The numerical approximations Y^1, Y^2 of (25a) and (25b), respectively, are the functions appearing in the averaging procedure to recover the macroscopic drift and diffusion functions (see (24a)-(24b)). Notice that we fix the slow variables in the system (25b) at the current macro state X_n. We use again the Euler–Maruyama method and compute Y^1, Y^2 as

$$Y^1_{n,\ell+1} = Y^1_{n,\ell} - \frac{\delta t}{\epsilon^2}\Lambda_M Y^1_{n,\ell} + \frac{\sqrt{\delta t}}{\epsilon}Q_M\boldsymbol{\xi}_n, \tag{26a}$$

$$Y^2_{n,\ell+1} = Y^2_{n,\ell} - \frac{\delta t}{\epsilon^2}\Lambda_M Y^2_{n,\ell} + \frac{\delta t}{\epsilon^2}\mathbf{b}\left(X_n, Y^1_{n,\ell}\right), \tag{26b}$$

where $\boldsymbol{\xi}_n = \mathrm{diag}(\xi_n^1,\dots,\xi_n^M)$ and ξ_n^k is a $\mathcal{N}(0,1)$ random variable. The index n refers to the macrotime, t_n. We compute (26a) over $L + L'$ microtime steps, (26b) over L microtime steps to compute the time-ensemble average (24a). Notice that for the microsolver, the timestep δt resolves the fine scale ϵ^2. The initial values for the micro solver are taken to be for $n \geqslant 1$

$$Y^1_{n,0} = Y^1_{n-1,\ell_T+L+L'-1}, \quad Y^2_{n,0} = Y^2_{n-1,\ell_T+L-1}$$

and $Y^1_{0,0} = Y^2_{0,0} = 0$ for $n = 0$. The motivation for computing the above time averages is given in the next section.

Remark 2.2. We notice that the auxiliary system (25) is degenerate, since the noise in (18b) is additive.[5] This implies that the results presented in [8, App. B] are not applicable in this case and a more elaborate analysis is required for proving geometric ergodicity. This analysis, based on the ergodic theory for hypoelliptic diffusions [30], will be presented elsewhere. In the present paper we will assume that the auxiliary process (25) is ergodic.

Advective time scale. A similar algorithm can be derived for the advective time scale. We consider the fast–slow system (5) that after projection and truncation reads

[5] Indeed, the auxiliary system in [29,8] will always be degenerate, whenever the noise in the fast/slow system of SDEs that we want to solve is additive.

$$\dot{\mathbf{x}} = \mathbf{a}(\mathbf{x},\mathbf{y}), \tag{27a}$$

$$\dot{\mathbf{y}} = -\frac{1}{\epsilon}\Lambda_M \mathbf{y} + \mathbf{b}(\mathbf{x},\mathbf{y}) + \frac{1}{\sqrt{\epsilon}}\mathbf{Q}_M \xi, \tag{27b}$$

similarly as (18). The macrosolver, chosen to be the Euler explicit method, is given by

$$X_{n+1} = X_n + \Delta t \mathbf{a}_M^n,$$

where the effective force $\mathbf{a}_M$ is given by the time average

$$\bar{\mathbf{a}}_M^n = \frac{1}{KL}\sum_{j=1}^{K}\sum_{\ell=\ell_T}^{\ell_T+L-1} \mathbf{a}(X_n, Y_{n,\ell j}), \tag{28}$$

where $Y_{n,\ell j}$ is a numerical approximation of the truncated fast system (37a) with a slow variable fixed at time t_n. As previously, K denotes the number of samples and L the number of micro timesteps and ℓ_T is the number of initial micro timestep ommited to reduce the transient effects. For the advective scaling, there is no need for an auxiliary problem for the micro solver [29].

3. Averaging and homogenization for SPDEs

In this section we summarize recent results on the averaging and homogenization for SPDEs [28,19] that are the analytical foundation on which the numerical algorithm presented in Section 2 is built.

3.1. Analytic form of the homogenized coefficients

In this section we briefly discuss the analytical form of the effective system corresponding to (18). Under the assumption that the vector field $\mathbf{a}_0(\mathbf{x},\mathbf{y})$ (see (21)) is centered with respect to the invariant measure of the fast process,

$$\int_{\mathbb{R}^M} \mathbf{a}_0(\mathbf{x},\mathbf{y})\mu(d\mathbf{y}) = 0, \tag{30}$$

then the slow process converges to a homogenized equation of the form

$$dX = \bar{\mathbf{a}}_M(X)dt + \bar{\boldsymbol{\sigma}}_M(X)dW, \tag{31}$$

where W represent an N-dimensional Wiener process and the SDE (31) is interpreted in the Itô sense. The subscript M are used to emphasise the fact that the homogenized coefficients depend on the number of fast processes that we take into account. An analytic expression for the coefficients that appear in (31) is given by

$$\bar{\mathbf{a}}_M(\mathbf{x}) = \lim_{\epsilon\to 0}\int_{\mathbb{R}^M\times\mathbb{R}^M} \nu_x^\epsilon(d\mathbf{y}^1, d\mathbf{y}^2)\nabla_y \mathbf{a}(\mathbf{x},\mathbf{y}^1)\mathbf{y}^2 + \lim_{\epsilon\to 0}\int_{\mathbb{R}^M}\mu(d\mathbf{y}^1)\int_0^{+\infty}\mathbb{E}_{y^1}\nabla_x \mathbf{a}(\mathbf{x},\mathbf{y}^1_{\epsilon^2 s})\mathbf{a}(\mathbf{x},\mathbf{y}^1)ds, \tag{32a}$$

$$\bar{\boldsymbol{\sigma}}_M(\mathbf{x})(\bar{\boldsymbol{\sigma}}_M(\mathbf{x}))^T = 2\lim_{\epsilon\to 0}\int_{\mathbb{R}^M}\mu(d\mathbf{y}^1)\mathbf{a}(\mathbf{x},\mathbf{y}^1)\otimes\int_0^{+\infty}\mathbb{E}_{y^1}\mathbf{a}(\mathbf{x},\mathbf{y}^1_{\epsilon^2 s})ds. \tag{32b}$$

Here $\mu(d\mathbf{y}_1)$ denotes the invariant measure of the process $\mathbf{y}^1$ which is given by (34) and $\nu_x^\epsilon(d\mathbf{y}^1, d\mathbf{y}^2)$ denotes the invariant measure of the the process $\{\mathbf{y}^1,\mathbf{y}^2\}$. Notice that $\mathbf{y}^1_{\epsilon^2 s} = \tilde{\mathbf{y}}^1_\tau$ is the solution of the rescaled process corresponding to (25a), i.e., $\dot{\tilde{\mathbf{y}}}^1 = -\Lambda_M\tilde{\mathbf{y}}^1 + Q_M\xi$. Alternatively, the calculation of the coefficients $\mathbf{a}_M(x)$ and $\boldsymbol{\sigma}_M(x)$ which appear in the homogenized equation can be obtained by the solution of the Poisson equation

$$-\mathcal{L}_M\phi = a_0(x,y), \tag{33}$$

where $\mathcal{L}_M$ is the generator of the fast (truncated) Ornstein–Uhlenbeck process. This process is ergodic and its invariant measure is Gaussian[6]:

$$\mu(d\mathbf{y}) = \frac{1}{\mathcal{Z}_{\mathcal{M}}}e^{-\sum_{j=1}^{M}\frac{\lambda_j y_j^2}{q_j^2}}d\mathbf{y}, \tag{34}$$

where $\mathcal{Z}_{\mathcal{M}}$ denotes the normalization constant. We notice that the system (18) is a finite dimensional fast–slow system of SDEs for which standard homogenization theory applies [26,27,25]. For quadratic nonlinearities the Poisson Eq. (33) can be solved analytically. The calculation of the coefficients in the homogenized (amplitude) equation reduces then to the calculation of Gaussian integrals that can also be done analytically. This will be done in Section 3.3.

[6] The notation used is explained in footnote 3 ; in particular, $\{\lambda_j\}_{j=1}^M$ and $\{q_j\}_{j=1}^M$ denotes the first M nonzero eigenvalues/noise intensities.

3.2. The advective time scale

Averaging problems for fast–slow systems of SPDEs were studied recently in [28] and their results can be applied to (5). One important observation is that in the system (5), the fast process is, to leading order $\mathcal{O}(1/\epsilon)$, an infinite dimensional Ornstein–Uhlenbeck process. The ergodic properties of such an infinite dimensional process can be analyzed in a quite straightforward way and the invariant measure, if it exists, is a Gaussian measure in an appropriate Hilbert space that can be written down explicitly [31,32].[7] Assuming that the process

$$\partial_t z = \mathcal{A}z + Q\xi \tag{35}$$

is ergodic with Gaussian invariant measure μ with mean 0 and covariance operator $\frac{1}{2}\mathcal{A}^{-1}Q^2$, $\mu \sim \mathcal{N}\left(0, \frac{1}{2}\mathcal{A}^{-1}Q^2\right)$ then the slow process x converges to the solution of the averaged equation

$$\dot{x} = \hat{a}(x), \quad \hat{a}(x) = \int a(x,y)\mu(dy), \tag{36}$$

where the integration is over an appropriate Hilbert space. See [Eqn. 5.2][28] and also [31,32] for background material on integration with respect to Gaussian measures.

When $F(\cdot)$ in (1) is given in terms of a symmetric bilinear map, i.e., $F(v) = B(v,v)$ the calculation of the vector field that appears in the averaged equation reduces to the calculation of Gaussian integrals and can be performed explicitly. In this case we have

$$\mathcal{P}_c B(x,y) := a(x,y) = D(x,x) + C(x,y) + E(y,y),$$

where

$$D_m(x,x) = \sum_{k,\ell=1}^{N} B_{k\ell m} x_k x_\ell,$$

$$C_m(x,y) = 2\sum_{k=1}^{N}\sum_{\ell=N+1}^{\infty} B_{k\ell m} x_k y_\ell,$$

$$E_m(x,y) = \sum_{k,\ell=N+1}^{\infty} B_{k\ell m} y_k y_\ell, \quad m = 1,\dots N$$

and where we used the notation $B_{k\ell m} := \langle B(e_k, e_\ell), e_m\rangle$ and $N := \dim(\mathcal{N})$ denotes the dimension of the null space of $\mathcal{A}$. Then, the fast–slow system (5) becomes

$$\dot{x} = D(x,x) + C(x,y) + E(y,y), \tag{37a}$$

$$\dot{y} = \frac{1}{\epsilon}\mathcal{A}y + b(x,y) + \frac{1}{\sqrt{\epsilon}}Q\xi \tag{37b}$$

and the averaged equation for (37) reads[8]

$$\dot{x} = D(x,x) + E, \tag{38}$$

where

$$E_m = \sum_{k=N+1}^{+\infty} \frac{q_k^2}{2\lambda_k} B_{kkm}, \quad m = 1,\dots N.$$

In the case when the null space is one-dimensional, $N = 1$, the averaged equation becomes

$$\dot{x} = DX^2 + E, \tag{39}$$

with $D = B_{111}$ and $E_m = \sum_{k=N+1}^{+\infty} \frac{q_k^2}{2\lambda_k} B_{kk1}$. This equation can be solved in closed form:

$$x(t) = \sqrt{\frac{E}{D}}\tan\left(\sqrt{ED}t + \arctan\left(\frac{Dx_0}{\sqrt{ED}}\right)\right).$$

We remark that solutions to (39), depending on the choice of the initial conditions, do not necessarily exist for all times. We also remark that it is straightforward to consider the case where there is an additional higher order linear term (in ϵ) in the equation, i.e. $F(v) = B(v,v) + \epsilon v v$ in the unscaled Eq. (1). In this case the averaged Eq. (38) becomes

$$\dot{x} = D(x,x) + vx + E,$$

where $x \in \mathbb{R}^N$.

[7] The analysis presented in [28] also applies to the case where the fast process is given by a semilinear parabolic SPDE. In this more general case, however, it is not possible to obtain an explicit formula for the invariant measure of the fast process.

[8] Notice that, in view of the fact that the invariant measure of (35) centered and independent of x, the linear term in y averages to 0 irrespective of the form of its dependence on x.

3.3. The diffusive time scale

We consider the system (4) obtained after a diffusive time rescaling to (1). In order to describe the homogenized equation, we further assume that $F(v)$ in (1) is of the form

$$F(v) = B(v, v) + \epsilon^2 v v, \tag{40}$$

where $B(\cdot,\cdot)$ is a symmetric bilinear map satisfying $\mathcal{P}_c B(e_k, e_k) = 0$.[9]

We recall that the noise does not act directly on the slow variables, $\langle Q\, e_k, e_k\rangle = 0$, $k = 1\ldots,N$, where N is the dimension of the null space of $\mathcal{A}$. Under appropriate assumptions on the quadratic nonlinearity and on the covariance operator of the noise, together with the assumptions on $\mathcal{A}$ and Q stated earlier in this section, it is possible to prove [19] that the projection of the solution to (4) onto the null space of $\mathcal{A}$, $x := \mathcal{P}_c u$, converges weakly to the solution of the homogenized SDE (the amplitude equation)

$$dX = \bar{\mathbf{a}}(X)dt + \bar{\boldsymbol{\sigma}}(X)dW(t), \quad X(0) = X_0, \tag{41}$$

where the noise is interpreted in the Itô sense and the drift $\bar{\mathbf{a}}(x)$ given by

$$\bar{\mathbf{a}}(x) = A_\infty x - B_\infty(x, x, x) + vx, \tag{42}$$

where the linear map $A_\infty : \mathcal{N} \to \mathcal{N}$ and the trilinear map $B_\infty : \mathcal{N}^3 \to \mathcal{N}$ are defined by

$$A_\infty x = 2B_c((I \otimes_s \mathcal{A})^{-1}(B_s \otimes_s I) + (I \otimes \mathcal{A}^{-1}B_s) + 2(B_c \otimes \mathcal{A}^{-1})))(x \otimes \widehat{Q}), \tag{43a}$$

$$B_\infty = -2B_c(x, c\mathcal{A}^{-1}B_s(x, x)). \tag{43b}$$

In the above we used the notation $B_s := \mathcal{P}_s B$ and $B_c := \mathcal{P}_c B$, whereas $\otimes_s$ stands for the symmetric tensor product[10] and where we have defined

$$\widehat{Q} = \sum_{k=N+1}^{\infty} \frac{q_k^2}{2\lambda_k}(e_k \otimes e_k).$$

The quadratic form associated with the diffusion matrix $\bar{\boldsymbol{\sigma}}^2$ is given by

$$\langle y, \bar{\boldsymbol{\sigma}}^2(x)y\rangle = 4\sum_{k=N+1}^{+\infty} q_k^2 \langle y, B_c(e_k, x)\rangle^2 + \sum_{k,\ell=N+1}^{+\infty} \frac{q_k^2 q_\ell^2}{2\lambda_\ell(\lambda_k + \lambda_\ell)} \langle y, B_c(e_k, e_\ell)\rangle^2. \tag{44}$$

Furthermore, the fast process can be approximated by an infinite dimensional Ornstein–Uhlenbeck process. The precise statement and proof of the above results can be found in [19].

Remark 3.1. The assumption that the $\mathcal{O}(\epsilon^2)$ term in (40) is linear is needed in order to go from (1) to (4) after rescaling or, equivalently, to (6). If our starting point is the already rescaled SPDE (4), then we can apply the results from [19] to nonlinearities of the form $F(v) = B(v, v) + \epsilon^2\, h(v)$ where $h(\cdot)$ is an arbitrary nonlinearity. In this case the drift term in the amplitude Eq. (42) becomes

$$\bar{\mathbf{a}}(x) = A_\infty x - B_\infty(x, x, x) + \int \mathcal{P}_c h(x, y)\mu(dy), \tag{45}$$

where $\mu(dy)$ denotes the invariant measure of the fast OU process.

When the null space of $\mathcal{A}$ is one dimensional and, consequently, the homogenized SDE is a scalar equation, it is possible to obtain sharp error estimates and to prove convergence in the strong topology. In this case Eq. (41) becomes

$$dX = \bar{a}(X)dt + \bar{\sigma}(X)dW, \quad X(0) = \langle u_0, e_1\rangle, \tag{46}$$

where

$$\bar{a}(X) = A_\infty X - B_\infty X^3, \quad \bar{\sigma}(X) = \sqrt{C_\infty + D_\infty X^2}. \tag{47}$$

[9] This is essentially the centering condition from homogenization theory, see Eq. (30) below.

[10] Given a Hilbert space $\mathcal{H}$ we denote by $\mathcal{H}\otimes_s\mathcal{H}$ its symmetric tensor product. Similarly, we use the notation $v_1 \otimes_s v_2 = \frac{1}{2}(v_1 \otimes v_2 + v_2 \otimes v_1)$ for the symmetric tensor product of two elements and $(A\otimes_s B)(x \otimes y) = \frac{1}{2}(Ax \otimes By + By \otimes Ax)$ for the symmetric tensor product of two linear operators. Furthermore, we extend the bilinear form B to the tensor product space by $B(u \otimes v) = B(u, v)$. More details can be found in [19, Section 4].

In the one dimensional case the formulas for the coefficients that appear in the homogenized equation have a simpler form than in the multidimensional case. In particular, we have, with $B_{k\ell m} = \langle B(e_k, e_\ell), e_m \rangle$:

$$A_\infty = \nu + \sum_{k=2}^{\infty} \frac{2B_{k11}^2 q_k^2}{\lambda_k^2} + \sum_{k,\ell=2}^{\infty} \frac{B_{k11}B_{\ell\ell k} q_\ell^2}{\lambda_k \lambda_\ell} + \sum_{k,\ell=2}^{\infty} \frac{2B_{k\ell 1}B_{k1\ell}}{\lambda_k + \lambda_\ell} \frac{q_k^2}{\lambda_k}, \tag{48a}$$

$$B_\infty = -\sum_{k=2}^{\infty} \frac{2B_{k11}B_{11k}}{\lambda_k}, \tag{48b}$$

$$C_\infty = \sum_{m,k=2}^{\infty} \frac{2B_{km1}^2 q_k^2 q_m^2}{(\lambda_k + \lambda_m)^2 \lambda_k}, \quad D_\infty = \sum_{k=2}^{\infty} \frac{4B_{k11}^2 q_k^2}{\lambda_k^2}. \tag{48c}$$

It is worth mentioning that if we are using a non-orthonormal basis, i.e. a basis $\hat{e}_k = c_k e_k$, then the coefficients that appear on the right hand side of the above equation transform according to

$$\widehat{B}_{k\ell m} = \frac{c_k c_\ell}{c_m} B_{k\ell m}. \tag{49}$$

We also have $\hat{q}_k = c_k q_k$.

Remark 3.2. The formulas for the coefficients that appear in the amplitude Eq. (41) can be also obtained by writing the SPDE (6) in Fourier space, truncating and then using singular perturbation theory-type of techniques for the corresponding backward Kolmogorov equation [33,34]. More details on this approach can be found in [35]. We also remark that, in general, both additive as well as multiplicative noise will appear in the amplitude equation, although only (degenerate) additive noise is present on the SPDE (1).

4. Numerical experiments

In this section we apply our numerical method to several SPDEs and report its convergence and performance. We consider here several examples of SPDEs with quadratic nonlinearities and check that the theory developed in [19] and summarized in Section 3 applies. For all of these examples we can derive rigorously the homogenized equation, with explicit formulas for the coefficients and therefore, we can present a rigorous numerical study for our algorithm and test the effectiveness of the proposed numerical algorithm.

4.1. Theoretical considerations

We will consider variants of the Burgers and the Kuramoto–Shivashinsky (KS) equations (with a linear instability term added) in one dimension with either Dirichlet or periodic boundary conditions. In particular, we will consider the singularly perturbed SPDEs (i.e. we have already rescaled to the diffusive time scale)

$$\partial_t u = \frac{1}{\epsilon^2}(\partial_x^2 + 1)u + \frac{1}{\epsilon} u \partial_x u + \nu u + \frac{1}{\epsilon} Q\xi \tag{50}$$

and

$$\partial_t u = \frac{1}{\epsilon^2}(-\partial_x^2 - \partial_x^4)u + \frac{1}{\epsilon} u \partial_x u + \nu u + \frac{1}{\epsilon} Q\xi, \tag{51}$$

respectively, where the noise ξ is as in Section 3. The operator Q, the covariance operator of the noise, has eigenvalues $\{q_k\}_{k=1}^{\infty}$ and eigenfunctions $\{e_k\}_{k=1}^{\infty}$, which are also the eigenfunctions of the differential operator that appears in either (50) or (51), i.e. the two operators commute. We will consider these two equations either on $[0,\pi]$ with Dirichlet boundary conditions or on $[-\pi,\pi]$ with periodic boundary conditions.

Remark 4.1. For the Burgers nonlinearity and for the boundary conditions that we consider it is straightforward to check that the centering condition $\mathcal{P}_c B(e_k, e_k) = 0$ is satisfied. A more natural equation to consider than (51) would be the KS equation in the small viscosity regime, i.e.

$$\partial_t u = \frac{1}{\epsilon^2}(-\partial_x^2 - \mu\partial_x^4)u + \frac{1}{\epsilon} u \partial_x u + \frac{1}{\epsilon} Q\xi,$$

where $\mu = 1 - \nu$, $\nu \in (0,1)$. This equation can be rewritten in the form

$$\partial_t u = \frac{1}{\epsilon^2}(-\partial_x^2 - \partial_x^4)u + \frac{1}{\epsilon} u \partial_x u + \nu\partial_x^4 u + \frac{1}{\epsilon} Q\xi. \tag{52}$$

The theory presented in [19] and the numerical scheme developed in this paper apply to this equation. The application of the numerical method developed in this paper to Eq. (52) and to related models will be presented elsewhere. Some recent analytical and numerical results on the behaviour of solutions to (52) have been reported in [20].

We will use the notation

$$\mathcal{A}_B = (\partial_x^2 + 1) \quad \text{and} \quad \mathcal{A}_{KS} = -\partial_x^2 - \partial_x^4.$$

It is possible to check that for the above equations and for the chose boundary conditions the theory developed in [19] and summarized in Section 3 applies. Consider first equations (50) and (51) on $[0,\pi]$ with Dirichlet boundary conditions. In this case the null space of $\mathcal{A}_B$ and $\mathcal{A}_{KS}$ is one dimensional:

$$\mathcal{N}(\mathcal{A}_*) = \text{span}\{\sin(\cdot)\}.$$

with $*$ being either B or KS. The normalized eigenfunctions of $\mathcal{A}_B$ and $\mathcal{A}_{KS}$ are $e_k = \sqrt{\frac{2}{\pi}}\sin(\pi k)$. The corresponding eigenvalues are

$$\lambda_k^B = k^2 - 1 \quad \text{and} \quad \lambda_k^{KS} = k^4 - k^2, \quad \text{for } k = 1, 2, \ldots.$$

Since the null space is one-dimensional, the homogenized equation is a scalar SDE. For the nonlinearity $B[u,v] = \frac{1}{2}\partial_x(uv)$ it is straightforward to calculate $B_{k\ell m} = \langle B(e_k, e_\ell), e_m\rangle$. We have

$$B_{k\ell m} = \frac{1}{2\sqrt{2\pi}}(|k+\ell|\delta_{k+\ell,m} - |k-\ell|\delta_{|k-\ell|,m}), \tag{53}$$

where $\delta_{k\ell}$ denotes the Kronecker delta. We can then use formulas (48) to calculate the formulas that appear in the homogenized equation. Let $\{-\lambda_k\}_{k=1}^{+\infty}$ of either $\mathcal{A}_B$ or $\mathcal{A}_{KS}$ with Dirichlet boundary conditions. The homogenized equation is given by (46) that we recall here for convenience

$$dX = \bar{a}(X)dt + \bar{\sigma}(X)dW, \tag{54}$$

where

$$\bar{a}(X) = A_\infty X - \frac{1}{4\lambda_2}X^3, \quad \bar{\sigma}(X) = \sqrt{2\left(\frac{q_2^2}{8\lambda_2^2}X^2 + C_\infty\right)}. \tag{55}$$

The coefficients that appear in (55) can be computed as[11]

$$A_\infty = \left(v + \frac{1}{8}\frac{q_2^2}{\lambda_2^2} + \frac{1}{8}\sum_{k=2}^{+\infty}\frac{k\lambda_k q_{k+1}^2 - \lambda_{k+1}q_k^2(k+1)}{(\lambda_{k+1}+\lambda_k)\lambda_k\lambda_{k+1}}\right), \tag{56a}$$

$$C_\infty = \left(\frac{1}{16}\sum_{k=2}^{+\infty}\frac{q_k^2 q_{k+1}^2}{\lambda_k\lambda_{k+1}(\lambda_k+\lambda_{k+1})}\right). \tag{56b}$$

In the case where only the second mode is forced with noise, $q_2 = \sigma$, $q_M = 0$, $M = 3,\ldots$ then the coefficients become

$$A_\infty = v + \frac{1}{8}\frac{\sigma^2}{\lambda_2^2} - \frac{3}{8}\frac{\sigma^2}{\lambda_2(\lambda_2+\lambda_3)}, \quad C_\infty = 0.$$

In this case only multiplicative noise appears in the homogenized equation and it can lead to intermittent behavior of solutions as well as noise induced transitions [20].

We will also consider either the Burgers or the KS equation on $[-\pi,\pi]$ with periodic boundary conditions. In this case the null space of both $\mathcal{A}_B$ and $\mathcal{A}_{KS}$ is two-dimensional and is spanned by

$$\mathcal{N}(\mathcal{A}_*) = \text{span}\{\sin(\cdot), \cos(\cdot)\},$$

with $*$ being either B or KS. The homogenized equation is given by (41), where $X = (X_1, X_2)$. It consists of a system of two coupled SDEs. We can use formulas (42) and (44), together with the formula for the nonlinearity $B[u,v] = \frac{1}{2}\partial_x(uv)$ to calculate the coefficients that appear in the homogenized equation.

4.2. Numerical experiments

We shall now apply our numerical algorithm to the model problems (50), (51) described in Section 4.1. As the behavior of our algorithm is similar for the Burgers and the Kuramoto–Shivashinsky equation we will do a thorough numerical study on the Burgers equation and comment on the results for the Kuramoto–Shivashinsky equation.

Burgers Equation. We consider Eq. (50) on $[0,\pi]$ with homogeneous Dirichlet boundary conditions. We know from Section 4.1 that, for ϵ sufficiently small, we have that

$$u(x,t) \approx X(t)\sin(x), \tag{57}$$

[11] We use the non-normalized basis $\hat{e}_k = \sin(\pi k)$ and use formula (49).

where $X(t)$ is the solution of (54). The precise statement of this result together with an error estimate can be found in [19, Thm. 7.1, Thm. 7.4]. The function $\bar{a}(X)$, $\bar{\sigma}(X)$ in (47) depends on A_∞, C_∞ which for the Burgers equation can be computed using formulas (56) with $\lambda_k = k^2 - 1$. They read $A_\infty = 0.0026744370$, $C_\infty = 0.0002659283$ (the fast convergence of the series (56) allows to compute numerically A_∞, C_∞ with high precision, given here up to ten digits). Following the algorithm described in Section (2), we look for a solution to (50) of the form

$$u(x,t) \simeq x(t)\sin(x) + \sum_{k=1}^{M} y_k(t)\sin(kx), \tag{58}$$

substitute the expansion in (50) to obtain the a fast–slow system of SDEs as described in (18). Following the algorithm of Section 2 we compute numerically the slow variable X_n as

$$X_{n+1} = X_n + \Delta t \bar{a}_M^n + \bar{\sigma}_M^n \Delta W_n, \tag{59}$$

where a_M^n, σ_M^n are given by (24a) and (24b), respectively. We also consider the truncated homogenized problem, i.e.,

$$dX = \bar{a}_M(X)dt + \bar{\sigma}_M(X)dW, \tag{60}$$

where

$$\bar{a}_M(X) = A_M X - \frac{1}{12}X^3, \quad \bar{\sigma}(X) = \sqrt{2\left(\frac{1}{72}X^2 + C_M\right)} \tag{61}$$

and where A_M, C_M, are obtained from (56a) and (56b) with the sums truncated at M. For numerical comparison we also compute

$$X_{n+1,\mathrm{inf}} = X_{n,\mathrm{inf}} + \Delta t \bar{a}(X_{n,\mathrm{inf}}) + \bar{\sigma}(X_{n,\mathrm{inf}})\Delta W_n, \tag{62}$$

$$X_{n+1,\mathrm{hom}} = X_{n,\mathrm{hom}} + \Delta t \bar{a}_M(X_{n,\mathrm{hom}}) + \bar{\sigma}_M(X_{n,\mathrm{hom}})\Delta W_n, \tag{63}$$

the Euler–Maruyama approximation of the SDEs (54) and (60), respectively. The same Brownian path will be used in (54), (59) and (60). We emphasize that the numerical solutions for (54) and (60) rely on analytically computed homogenized coefficients, whereas for (59) we implement the multiscale algorithm of Section 2, where the coefficients a_M^n, σ_M^n are computed "on the fly" and rely on the microsolver (26a) and (26b). Hence no a-priori analytical knowledge of the amplitude equation is required.

We choose the values of the various parameters entering in the averaging process for the computation of $\bar{a}_M^n$, $\bar{\sigma}_M^n$ as suggested in [8], i.e., $K = 1$, $\delta t/\epsilon^2 = \mathcal{O}(2^{-p})$, $n_T = \mathcal{O}(1)$, $L = \mathcal{O}(2^{3p})$, $L' = \mathcal{O}(p \cdot 2^p)$. According to [8], this guarantees (for the case of non-degenerate fast processes) that the error is bounded by 2^{-p}. In our case with a degenerate fast process an error bound is still to be established. Here we monitor such convergence numerically. More precisely, we set $n_T = 16$, $L = 2^{3p}$, $L' = p \cdot 2^p$ and monitor the error using

$$E_p^M = \frac{1}{N}\sum_{n=1}^{N}\left(\left|\bar{a}_M^n - \bar{a}_M(X_{n,\mathrm{hom}})\right| + \left|\bar{\sigma}_M^n - \bar{\sigma}_M(X_{n,\mathrm{hom}})\right|\right), \tag{64a}$$

$$E_{l,p}^M = \frac{1}{N}\sum_{n=1}^{N}\left(\left|\bar{a}_M^n - \bar{a}(X_{n,\mathrm{inf}})\right| + \left|\bar{\sigma}_M^n - \bar{\sigma}(X_{n,\mathrm{hom}})\right|\right) \tag{64b}$$

for various values of p, where $\Delta t = T/N$ and T represent the final time. Notice that (64a) captures the error between (60)–the homogenized solution of the truncated system–and the numerical solution of the truncated system, while (64b), where the index l stands for limit, captures the error between the homogenized solution of the limit problem (54) and the numerical solution of the truncated system.

2-mode truncation. We set $M = 2$ in (58) and substitute the expansion in (50) to obtain the following system of equations

$$\dot{x} = \nu x - \frac{1}{2\epsilon}(xy_1 + y_1y_2), \tag{65a}$$

$$\dot{y}_1 = \left(\nu - \frac{3}{\epsilon^2}\right)y_1 - \frac{1}{\epsilon}\left(xy_2 - \frac{1}{2}x^2\right) + \frac{q_1}{\epsilon}\xi_1(t), \tag{65b}$$

$$\dot{y}_3 = \left(\nu - \frac{8}{\epsilon^2}\right)y_2 + \frac{3}{2\epsilon}(xy_1) + \frac{q_2}{\epsilon}\xi_2(t). \tag{65c}$$

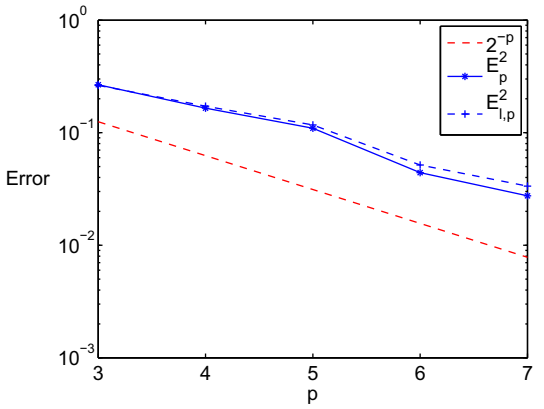

Fig. 1. Numerical convergence for 2-mode truncation. On the horizontal axis we monitor the accuracy of the micro-timestep and on the vertical axis we measure the error as given by (64a) and (64b) with $M = 2$.

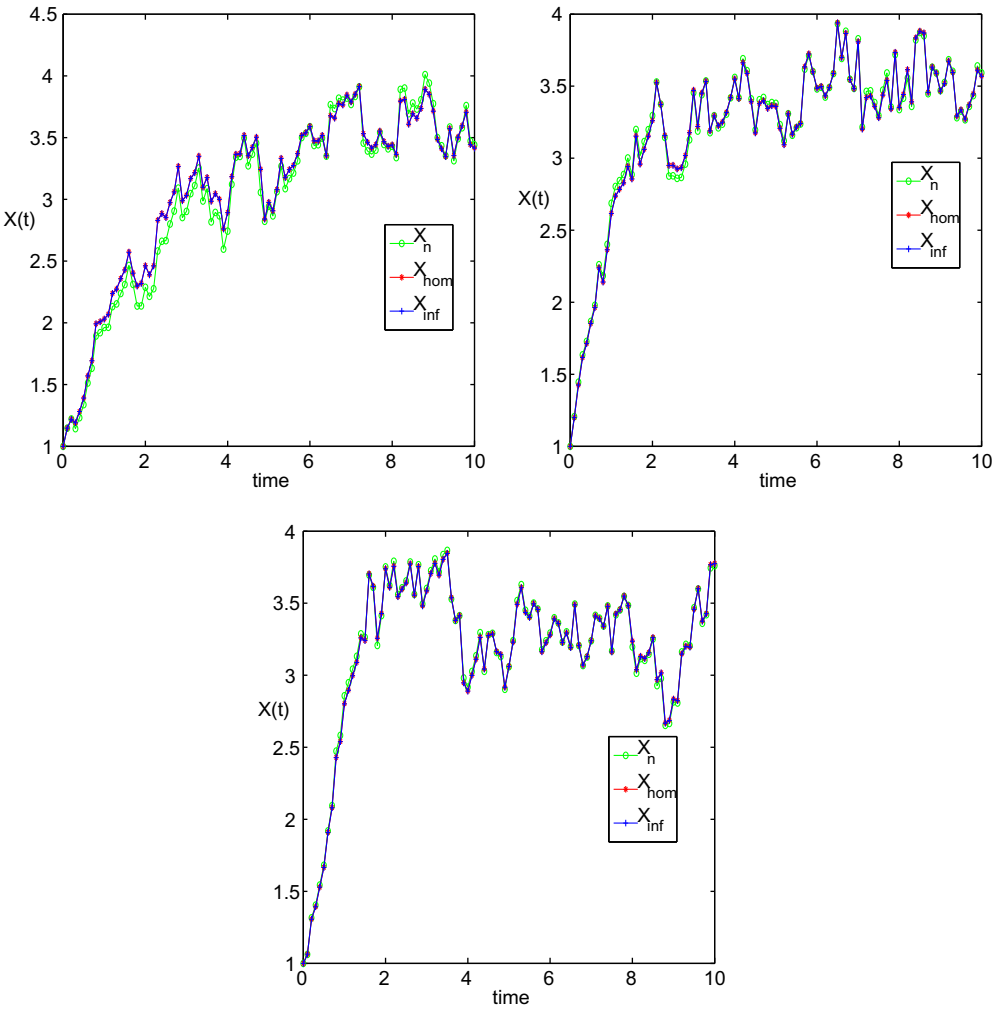

Fig. 2. Euler–Maruyama methods (59) (solution denoted X_n), (63) (solution denoted $X_{n,\mathrm{hom}}$) and (62) (solution denoted $X_{n,\mathrm{inf}}$) for three paths (upper panel, left $p = 3$ for X_n, upper panel right $p = 4$ for X_n, lower panel $p = 5$ for X_n). We use 2-mode truncation for (59) and (63).

The auxiliary process can be derived as explained in Section 2 and reads

$$\dot{y}_1^1 = -\frac{3}{\epsilon^2} y_1^1 + \frac{q_1}{\epsilon}\xi_1(t), \tag{66a}$$

$$\dot{y}_2^1 = -\frac{8}{\epsilon^2} y_2^1 + \frac{q_2}{\epsilon}\xi_2(t), \tag{66b}$$

$$\dot{y}_1^2 = -\frac{3}{\epsilon^2} y_1^2 - \frac{1}{\epsilon^2}\left(x y_2^1 - \frac{x^2}{2}\right), \tag{66c}$$

$$\dot{y}_2^2 = -\frac{8}{\epsilon^2} y_2^1 + \frac{3}{2\epsilon^2} x y_1^1. \tag{66d}$$

We apply the algorithm of Section 2 to get a numerical approximation of the homogenised problem corresponding to (65). The final time is $T = 1$ and $N = 10$, which corresponds to macro time-step of size $\Delta t = 0.1$. The macro solver for the method is given by (59). As mentioned above, we compare our results with (62) and (63). The unknown coefficients A_3, C_3 in (61) can be computed using (56a) and (56b), where the sum is truncated at $M + 1 = 3$ and read $A_3 = 0.003735726834$, $C_3 = 0.0002593873518$.

We observe in Fig. 1 that we get numerically the expected order of convergence corresponding to $\delta t/\epsilon^2 = \mathcal{O}(2^{-p})$. Furthermore, as the micro time-step becomes smaller, the numerical scheme gets closer to (59) and slightly deviates from (54). This is expected as the numerical solution is not converging to that latter solution. We observe nevertheless that with only two fast modes, the numerical scheme already captures quite well the effective behavior of the slow variable of the infinite dimensional system.

We also illustrate the time evolution of one trajectory comparing over the time $0 \leqslant t \leqslant T$ with $T = 10$, the Euler–Maruyama method for the amplitude Eq. (62), the homogenized Eq. (63) and the macro solver (59). The same Brownian path is used for generating the three trajectories and as well as the same macro time step. We perform this comparison for increasing accuracy of the micro solver used to recover the macro data, namely, $\delta t/\epsilon^2 = \mathcal{O}(2^{-p})$, $p = 3, 4, 5$. We see in Fig. 2 that the trajectory for the amplitude equation and the homogenized equation coincide, while the macro solver gets closer to the true dynamics as we refine the micro time step. For the same trajectory we also give in Fig. 3 a space-time plot for the approximation of the original SPDE $u(\cdot,t) \approx X(t)\sin(\cdot)$, with $X(t)$ solution of the amplitude equation, the homogenized equation or the macro solver. Again we see that the numerical method captures the right behavior of the solution.

3-mode truncation. We set $M = 3$ in (58) and obtain the following system of equations

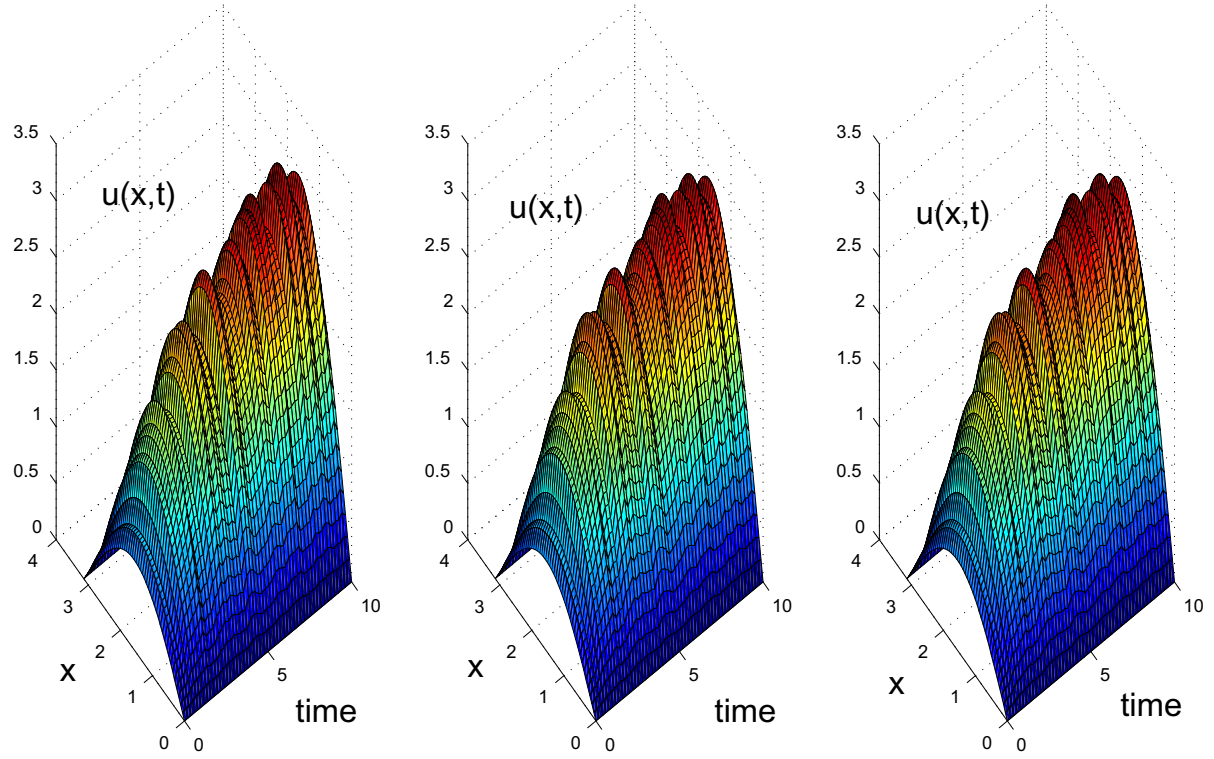

Fig. 3. Approximation (57) of the solution $u(x,t)$ of the SPDE; $u(\cdot,t) \simeq X_n(t)\sin(\pi\cdot)$ (left figure $p = 3$), $u(\cdot,t) \simeq X_{n,\mathrm{hom}}(t)\sin(\pi\cdot)$ (middle figure) and $u(\cdot,t) \simeq X_{n,\mathrm{inf}}(t)\sin(\pi\cdot)$ (right figure).

$$\dot{x} = \nu x - \frac{1}{2\epsilon}(xy_1 + y_1y_2 + y_2y_3), \tag{67a}$$

$$\dot{y}_1 = \left(\nu - \frac{3}{\epsilon^2}\right)y_1 - \frac{1}{\epsilon}\left(xy_2 + y_1y_3 - \frac{1}{2}x^2\right) + \frac{q_1}{\epsilon}\xi_1(t), \tag{67b}$$

$$\dot{y}_2 = \left(\nu - \frac{8}{\epsilon^2}\right)y_2 - \frac{3}{2\epsilon}(xy_3 - xy_1) + \frac{q_2}{\epsilon}\xi_2(t), \tag{67c}$$

$$\dot{y}_3 = \left(\nu - \frac{15}{\epsilon^2}\right)y_3 + \frac{1}{\epsilon}(2xy_2 + y_1^2) + \frac{q_3}{\epsilon}\xi_3(t). \tag{67d}$$

The auxiliary process can be computed similarly as for the 2-mode truncation. We perform the same set of numerical experiments as for the 2-mode truncation, reported in Fig. 4. Similar behavior than previously noted can be observed. Observe that the discrepancy between the numerical scheme and (54) gets smaller. This is expected as with additional modes, the homogenized Eq. (60) (that we aim at approximating with our multiscale scheme) gets closer to (54).

4-mode truncation. We set $M = 4$ in (58) and apply the similar procedure as previously. For the sake of brevity, we do not write the system of equations in this case and just report the numerical convergence.

We see in Fig. 5 a similar behavior of our numerical scheme as observed previously. We again notice that the discrepancy between the numerical scheme and (54) is smaller than for lower order truncation. We also notice that for the auxiliary process, one of the SDE reads $\dot{y}_4 = (\nu - \frac{24}{\epsilon^2})y_4 + \dots$ As we solve the auxiliary process with the explicit Euler–Maruyama scheme, we have a stepsize restriction of the type $24\delta t/\epsilon^2 \leqslant 2$ to ensure boundedness of the (micro) numerical solution (see e.g., [36, Section 4.2]). Thus, the micro-timesteps 2^{-p}, $p \leqslant 3$ cannot be used and we therefore only report numerical results for micro-timesteps 2^{-p}, $p \geqslant 4$.

The Kuramoto–Shivashinsky equation. The equations for the M-mode truncation of the Kuramoto–Shivashinsky equation are very similar to the ones for the Burgers equation and will not be presented here. The only difference is that the fast process is more dissipative than for the Burgers equation, due to the stronger dissipativity of the operator $\mathcal{A}_{KS}$ compared

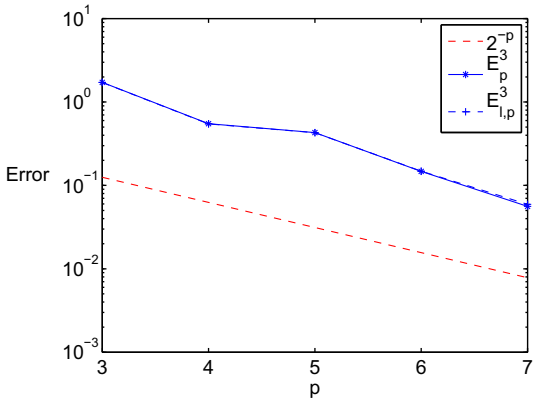

Fig. 4. Numerical convergence for 3-mode truncation. On the horizontal axis we monitor the accuracy of the micro-timestep and on the vertical axis we measure the error as given by (64a) and (64b) with $M = 3$.

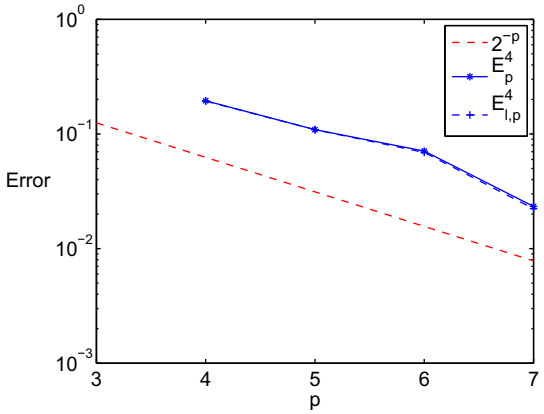

Fig. 5. Numerical convergence for 4-mode truncation. On the horizontal axis we monitor the accuracy of the micro-timestep and on the vertical axis we measure the error as given by (64a) and (64b) with $M = 4$.

to $\mathcal{A}_B$. As the results of the numerical experiments for the KS equation are very similar to the results reported in this section for the Burgers equation, they will not be presented here.

5. Conclusions and further work

We have presented a new numerical method for the efficient and accurate solution of stochastic partial differential equations with multiple scales. The new numerical scheme is based on a combination of a spectral method with the HMM methodology and has been tested on SPDEs with quadratic nonlinearities for which a rigorous homogenization theory exists. This enables us to check the performance of our method. The numerical experiments presented in this paper suggest that the new method performs well and allows to solve accurately multiscale SPDEs by solving a low dimensional fast–slow system of SDEs. The method is suitable for infinite dimensional stochastic systems for which there is clear separation of scales, and for which a low dimensional homogenised (or averaged) equation for the slow modes exists.

There are still many questions that are left open. First, the rigorous analysis of the proposed method and a careful study of the convergence and stability properties of the proposed method remains to be done. In addition, the optimisation of the proposed method by tuning appropriately the parameters of the algorithm has not been performed yet. This appears to be an open problem even when the HMM methodology is applied to finite dimensional fast/slow systems of SDEs [37].

The proposed numerical algorithm could be used to study in detail the qualitative and quantitative properties of solutions to SPDEs with quadratic nonlinearities, since SPDEs of this form exhibit very rich dynamical behaviour. Furthermore, we would like to apply the numerical algorithm to more general classes (and systems) of semilinear SPDEs, for which an averaged or homogenised equation is known to exist. Examples include systems of reaction/diffusion equations that were considered in [28] as well as the Swift–Hohenberg SPDE [38].

In our algorithm, we did not make use of the fact that the form of the amplitude equation (i.e. a Landau equation with additive and multiplicative noise) is known. Knowledge of the functional form of the coefficients that appear in the homogenised or averaged equation can be used in order to simplify the numerical algorithm. The stochastic Landau equation appears as the amplitude equation for several infinite dimensional stochastic dynamical systems, not only for SPDEs with quadratic nonlinearities, e.g. [39]. Thus, the algorithm proposed in this paper, could be modified to develop an efficient method for studying the dynamics of SPDEs near bifurcation. All these topics are currently under investigation.

Acknowledgments

Part of this work was done while GP was visiting the Mathematics Section of EPFL. The hospitality of the department and of the group of A. Abdulle is greatly acknowledged. The authors thank S. Krumscheid for an extremely careful reading of an earlier version of the paper and for many useful remarks. GP is supported by the EPSRC. The work of AA was supported in part by the Swiss National Science Foundation under Grant 200021 134716.

References

[1] A.J. Majda, C. Franzke, B. Khouider, An applied mathematics perspective on stochastic modelling for climate, Philos. Trans. R. Soc. Lond. Ser. A Math. Phys. Eng. Sci. 366 (1875) (2008) 2429–2455, doi:10.1098/rsta.2008.0012. <http://dx.doi.org/10.1098/rsta.2008.0012>.
[2] M. Griebel, S. Knapek, G. Zumbusch, Numerical Simulation in Molecular Dynamics, Texts in Computational Science and Engineering, vol. 5, Springer, Berlin, 2007. numerics, algorithms, parallelization, applications..
[3] J. Fish, Multiscale Methods: Bridging The Scales In Science and Engineering, Oxford University Press, Oxford, 2009.
[4] A. Einstein, Investigations on the theory of the Brownian movement, Dover Publications Inc., New York, 1956, edited with notes by R. Fürth, Translated by A.D. Cowper.
[5] W. Horsthemke, R. Lefever, Noise-induced Transitions, Springer Series in Synergetics, vol. 15, Springer-Verlag, Berlin, 1984. theory and applications in physics, chemistry, and biology..
[6] R. Mazo, Brownian Motion, International Series of Monographs on Physics, vol. 112, Oxford University Press, New York, 2002.
[7] R. Zwanzig, Nonequilibrium Statistical Mechanics, Oxford University Press, New York, 2001.
[8] W. E, D. Liu, E. Vanden-Eijnden, Analysis of multiscale methods for stochastic differential equations, Commun. Pure Appl. Math. 58 (11) (2005) 1544–1585.
[9] L.D. Landau, E.M. Lifshitz, Fluid mechanics, Translated from the Russian by J.B. Sykes and W.H. Reid. Course of Theoretical Physics, vol. 6, Pergamon Press, London, 1959.
[10] M.C. Cross, P.C. Hohenberg, Pattern formation outside of equilibrium, Rev. Mod. Phys. 65 (1993) 851–1112, doi:10.1103/RevModPhys.65.851. <http://link.aps.org/doi/10.1103/RevModPhys.65.851>.
[11] M. Hairer, A.M. Stuart, J. Voss, Analysis of SPDEs arising in path sampling. II. The nonlinear case, Ann. Appl. Probab. 17 (56) (2007) 1657–1706, doi:10.1214/07-AAP441. <http://dx.doi.org/10.1214/07-AAP441>.
[12] A. Alabert, I. Gyöngy, On numerical approximation of stochastic Burgers' equation, in: From Stochastic Calculus to Mathematical Finance, Springer, Berlin, 2006, pp. 1–15.
[13] A.M. Davie, J.G. Gaines, Convergence of numerical schemes for the solution of parabolic stochastic partial differential equations, Math. Comput. 70 (233) (2001) 121–134 (electronic).
[14] J. Printems, On the discretization in time of parabolic stochastic partial differential equations, M2AN Math. Model. Numer. Anal. 35 (6) (2001) 1055–1078.
[15] T. Li, A. Abdulle, W. E, Effectiveness of implicit methods for stiff stochastic differential equations, Commun. Comput. Phys. 3 (2) (2008) 295–307.
[16] A. Abdulle, S. Cirilli, Stabilized methods for stiff stochastic systems, C.R. Math. Acad. Sci. Paris 345 (10) (2007) 593–598, doi:10.1016/j.crma.2007.10.009. <http://dx.doi.org/10.1016/j.crma.2007.10.009>.
[17] A. Abdulle, S. Cirilli, S-ROCK: Chebyshev methods for stiff stochastic differential equations, SIAM J. Sci. Comput. 30 (2) (2008) 997–1014, doi:10.1137/070679375. <http://dx.doi.org/10.1137/070679375>.

[18] A. Abdulle, T. Li, S-ROCK methods for stiff ItôSDEs, Commun. Math. Sci. 6 (4) (2008) 845–868. <http://projecteuclid.org/getRecord?id=euclid.cms/1229619673>.
[19] D. Blömker, M. Hairer, G.A. Pavliotis, Multiscale analysis for stochastic partial differential equations with quadratic nonlinearities, Nonlinearity 20 (7) (2007) 1721–1744.
[20] M. Pradas, D. Tseluiko, S. Kalliadasis, D.T. Papageorgiou, G.A. Pavliotis, Noise induced state transitions, intermittency, and universality in the noisy Kuramoto–Sivashinksy equation, Phys. Rev. Lett. 106 (6) (2011) 060602, doi:10.1103/PhysRevLett.106.060602.
[21] M. Kardar, G. Parisi, Y.-C. Zhang, Dynamic scaling of growing interfaces, Phys. Rev. Lett. 56 (9) (1986) 889–892, doi:10.1103/PhysRevLett.56.889.
[22] S. Zaleski, A stochastic model for the large scale dynamics of some fluctuating interfaces, Phys. D 34 (3) (1989) 427–438, doi:10.1016/0167-2789(89)90266-2. <http://dx.doi.org/10.1016/0167-2789(89)90266-2>.
[23] X. Wan, X. Zhou, W. E, Study of the noise-induced transition and the exploration of the phase space for the Kuramoto–Sivashinsky equation using the minimum action method, Nonlinearity 23 (3) (2010) 475–493, doi:10.1088/0951-7715/23/3/002. <http://dx.doi.org/10.1088/0951-7715/23/3/002>.
[24] D. Blömker, M. Hairer, G. Pavliotis, Some remarks on stabilization by additive noise, Preprint.
[25] G. Pavliotis, A. Stuart, Multiscale Methods of Texts in Applied Mathematics, vol. 53, Springer, New York, 2008 (averaging and homogenization).
[26] A. Bensoussan, J.-L. Lions, G. Papanicolaou, Asymptotic analysis for periodic structures, Studies in Mathematics and its Applications, vol. 5, North-Holland Publishing Co., Amsterdam, 1978.
[27] G.C. Papanicolaou, D. Stroock, S.R.S. Varadhan, Martingale approach to some limit theorems, in: Papers from the Duke Turbulence Conference (Duke Univ., Durham, N.C., 1976), Paper No. 6, Duke Univ., Durham, N.C., 1977, pp. ii+120 pp. Duke Univ. Math. Ser., vol. III.
[28] S. Cerrai, M. Freidlin, Averaging principle for a class of stochastic reaction–diffusion equations, Probab. Theory Related Fields 144 (1-2) (2009) 137–177.
[29] E. Vanden-Eijnden, Numerical techniques for multi-scale dynamical systems with stochastic effects, Commun. Math. Sci. 1 (2) (2003) 385–391.
[30] J. Mattingly, A.M. Stuart, Geometric ergodicity of some hypo-elliptic diffusions for particle motions, Markov Process. Related Fields 8 (2) (2002) 199–214.
[31] G.D. Prato, J. Zabczyk, Stochastic equations in infinite dimensions, Encyclopedia of Mathematics and its Applications, vol. 44, Cambridge University Press, Cambridge, 1992.
[32] G. Da Prato, J. Zabczyk, Ergodicity for Infinite-Dimensional Systems, London Mathematical Society Lecture Note Series, vol. 229, Cambridge University Press, Cambridge, 1996, doi:10.1017/CBO9780511662829. <http://dx.doi.org/10.1017/CBO9780511662829>.
[33] T. Kurtz, A limit theorem for perturbed operator semigroups with applications to random evolutions, J. Funct. Anal. 12 (1973) 55–67.
[34] G.C. Papanicolaou, Some probabilistic problems and methods in singular perturbations, Rocky Mount. J. Math. 6 (4) (1976) 653–674.
[35] A. Majda, I. Timofeyev, E.V. Eijnden, A mathematical framework for stochastic climate models, Commun. Pure Appl. Math. 54 (8) (2001) 891–974.
[36] E. Hairer, G. Wanner, Solving Ordinary Differential Equations II. Stiff and Differential-Algebraic Problems, Second ed., Springer, Verlag, 1996.
[37] D. Liu, Optimal error estimates for heterogeneous multiscale methods for stochastic dynamical systems, Preprint.
[38] D. Blömker, M. Hairer, G.A. Pavliotis, Modulation equations: stochastic bifurcation in large domains, Commun. Math. Phys. 258 (1) (2005) 479–512.
[39] D. Blömker, S. Maier-Paape, G. Schneider, The stochastic Landau equation as an amplitude equation, Discrete Contin. Dyn. Syst. Ser. B 1 (4) (2001) 527–541, doi:10.3934/dcdsb.2001.1.527. <http://dx.doi.org/10.3934/dcdsb.2001.1.527>.